





Article

Drought-Adaptive Mechanisms of Young Sweet Cherry Trees in Response to Withholding and Resuming Irrigation Cycles

Pedro José Blaya-Ros ¹, Víctor Blanco ¹, Roque Torres-Sánchez ² and Rafael Domingo ^{1,*}

¹ Dpto Ingeniería Agronómica, Universidad Politécnica de Cartagena (UPCT), Paseo Alfonso XIII, 48, E-30203 Cartagena, Spain; pedro.blaya@upct.es (P.J.B.-R.); victor.blanco@wsu.edu (V.B.)

² Dpto Automática, Ingeniería Eléctrica y Tecnología Electrónica, Universidad Politécnica de Cartagena (UPCT), Campus de la Muralla s/n, E-30202 Cartagena, Spain; roque.torres@upct.es

* Correspondence: rafael.domingo@upct.es; Tel.: +34-968-32-54-45

Abstract: The present work evaluates the main adaptive mechanisms developed by young sweet cherry trees (*Prunus avium* L.) to cope with drought. For this purpose, the young trees were subjected to two drought cycles with different water stress intensities followed by a recovery period. Three irrigation treatments were applied: control treatment (CTL) irrigated to ensure non-limiting soil water conditions; moderate water stress (MS) subjected to two drying cycles whose duration was dependent on the time elapsed until the trees reached values of midday stem water potential (Ψ_{stem}) of -1.3 and -1.7 MPa for the first and second cycle, respectively; and severe water stress (SS) similar to MS, but with reference values of -1.6 and -2.5 MPa. In-between drought cycles, MS and SS trees were irrigated daily as the CTL trees until reaching Ψ_{stem} values similar to those of CTL trees. The MS and SS trees showed an important stomatal regulation and lower vegetative growth. The decreasing leaf turgor potential (Ψ_{turgor}) during the drought periods accounted for 40–100% of the reduction in leaf water potential at midday (Ψ_{md}). The minimum osmotic potential for mature leaves was about 0.35 MPa lower than in well-irrigated trees. The occasional osmotic adjustment observed in MS and SS trees was not sufficient to maintain Ψ_{turgor} values similar to the CTL trees or to increase the specific leaf weight (SLW). The leaf insertion angle increased as the water stress level increased. Severe water stress ($\Psi_{\text{stem}} < -2.0$ MPa) resulted in clear early defoliation as a further step in water conservation.

Keywords: leaf insertion angle; leaf water potential and components; *Prunus avium* L.; water stress; stem water potential; vegetative growth; defoliation



Citation: Blaya-Ros, P.J.; Blanco, V.; Torres-Sánchez, R.; Domingo, R. Drought-Adaptive Mechanisms of Young Sweet Cherry Trees in Response to Withholding and Resuming Irrigation Cycles. *Agronomy* **2021**, *11*, 1812. <https://doi.org/10.3390/agronomy11091812>

Academic Editor: Alejandro Galindo

Received: 27 July 2021

Accepted: 7 September 2021

Published: 9 September 2021

Publisher's Note: MDPI stays neutral with regard to jurisdictional claims in published maps and institutional affiliations.



Copyright: © 2021 by the authors. Licensee MDPI, Basel, Switzerland. This article is an open access article distributed under the terms and conditions of the Creative Commons Attribution (CC BY) license (<https://creativecommons.org/licenses/by/4.0/>).

1. Introduction

In drylands, where scarce water availability is the main restricting factor for crops, drought periods have increased in terms of the geographic area affected, frequency, and intensity as a consequence of global climate change [1]. Drought stress, generally characterized by a combination of high solar radiation, high temperature, and water scarcity [2], is one of the main abiotic stresses worldwide that negatively affects crops' metabolism, growth, and yield [3]. In these areas, even under irrigated agricultural conditions, crops may be subjected to many instances of stress and recovery from cycle stress [4]. In this context, it is indispensable to understand how a plant responds and adapts to drought conditions in order to maintain its growth, development, and productivity. The adaptive responses of plants to drought can be morphological, physiological, or biochemical and are not easy to understand, as they are dependent on the plant type, phenological stage, stress duration, intensity, and rate of stress imposition and frequency [5]. For this reason, understanding the mechanisms involved in a crop's responses and adaptations to drought periods is essential for the successful implementation of deficit irrigation strategies to minimize the damages caused to yield and fruit quality [6] and to cope with increasingly frequent drought periods.

Sweet cherry trees (*Prunus avium* L.) are amongst the most important fruit trees grown commercially worldwide. The world production of fresh cherries has increased by 29% in the last 10 years, reaching 2.6 Mt in 2019 [7]. Spain is the sixth-largest worldwide producer and the largest producer of fresh cherries in Europe [7]. Sweet cherry trees are characterized by their significant sensitivity to water stress during preharvest, when fruit growth may be penalized by water deficit [8–10]. Conversely, water deficit could be applied during the post-harvest period, after the flower differentiation period, when fruit quality or yield is little or not penalized by regulated water deficit [11]. In this way, deficit irrigation strategies have been successfully applied to sweet cherry trees [8,10–12]. However, there is still a lack of knowledge on the drought adaptation mechanisms of sweet cherry trees, with this knowledge being decisive for the management of sweet cherry orchards under regulated deficit irrigation (RDI).

The mechanisms developed by crops to resist water deficit can be divided into escape, avoidance, or tolerance [13]. Thus, in the genus *Prunus*, certain morphological and physiological adaptations allow its species to survive in situations of water stress [14,15]. Previous studies with almond and apricot trees indicated that drought adaptations were mainly based on avoidance mechanisms [14,16]. Stomatal control is considered the main physiological mechanism for regulating transpiration and conserving water in plants to avoid irreversible damage due to dehydration [17]. In this context, strong stomatal regulation was described in young and mature sweet cherry trees under water stress [18,19]. These mechanisms allow the plants to minimize water loss and maximize water uptake. Likewise, drought stress could modify the morphology of the leaf (e.g., leaf size and thickness) and reduce vegetative growth, which, together with stomatal regulation, would lead to a significant decrease in photosynthesis [17,20]. Livellara et al. [21] reported a significant reduction in shoot length and canopy volume in young sweet cherry trees. On the other hand, tolerance mechanisms, such as the active accumulation of osmotically active solutes, have been reported for many crops [22]. An increase in the concentration of solutes could contribute to a reduction in the osmotic potential, thereby maintaining the turgor potential in the cells [22], although the capacity for osmotic adjustment may vary among organs within a plant [23]. In almond trees, Castel and Fereres [14] reported that the degree of osmotic adjustment was limited during water stress periods, with the trees unable to maintain high turgor potential values.

Despite the importance and cost-effectiveness in cherry tree cultivation [10], the drought-adaptive mechanisms developed by this crop to water stress have been poorly studied. We hypothesize that sweet cherry trees can develop adaptive mechanisms to water stress that makes them capable of maintaining cell turgor and therefore turgor-dependent processes and that knowledge of these adaptive mechanisms is of great interest for the design of regulated deficit irrigation strategies under our growing conditions. For this reason, the purpose of the study is to increase our understanding of the responses of sweet cherry trees to water deficit and to describe the avoidance and tolerance mechanisms developed in response to two withholding and resuming irrigation cycles of different duration and intensity during post-harvest, a non-critical period for sweet cherry trees.

2. Materials and Methods

2.1. Study Site

The trial was carried out during two consecutive summers (2018 and 2019) at the UPCT “Tomás Ferro” experimental orchard in Cartagena, Spain (37°41' N, 0°57' W, 32 m altitude), using three-year-old ‘Lapins’ sweet cherry trees grafted onto ‘Mirabolano’ rootstock with a tree spacing of 3.5 × 2.25 m. The soil, with a bulk density of 1.4 ± 0.1 g cm⁻³, had a sandy-clay-loam texture (34.5%, 21.3%, and 44.2% clay, silt, and sand particle size, respectively) with a low organic matter content (1.5%). The drip irrigation system consisted of a single drip line per row of trees with 3 pressure-compensated drippers per tree with a nominal emitter discharge of 2.2 L h⁻¹. The irrigation water was sourced from the Tajo-Segura Water Transfer System. It had an average electrical conductivity at 25 °C of 1.1 dS m⁻¹,

low salinity, a pH of 7.90, and average levels of chloride and sodium contents of 1.03 and 1.66 meq L⁻¹, respectively.

Daily meteorological data were recorded by an automated weather station (CA52) installed close to the experimental orchard (≈ 300 m) owned by the Agricultural Information Network System of Murcia (SIAM 2020—<http://siam.imida.es/>, accessed on 13 January 2020). The reference crop evapotranspiration (ET₀) was calculated using the Penman–Monteith equation [24], and the daily mean air vapor pressure deficit (VPD) was calculated using air temperature and relative humidity data [24]. Crop evapotranspiration (ET_c) was estimated weekly from mid-May to early November according to the methodology proposed by Allen et al. [24]. The crop coefficient (K_c) used was based on Marsal [25] and ranged from 0.3 to 0.96, and the evaporation reduction coefficient (K_r) used was based on Fereres [26].

The weather was typically a semi-arid Mediterranean-type climate, characterized by hot, dry summers and wet, mild winters. Both years had similar seasonal weather patterns (Figure 1). The VPD reached daily mean values in summer of 2.69 and 3.09 kPa in 2018 and 2019, respectively. The seasonal evolution of ET₀ values oscillated between 0.53 and 7.73 mm d⁻¹, and the cumulative values of ET₀ were 1308 and 1261 mm in 2018 and 2019, respectively. Annual rainfall was mainly recorded in spring and autumn, with a total of 338 and 479 mm in 2018 and 2019, respectively. In September 2019, 202.6 mm (42.3% of total) of rainfall accumulated in four consecutive days.

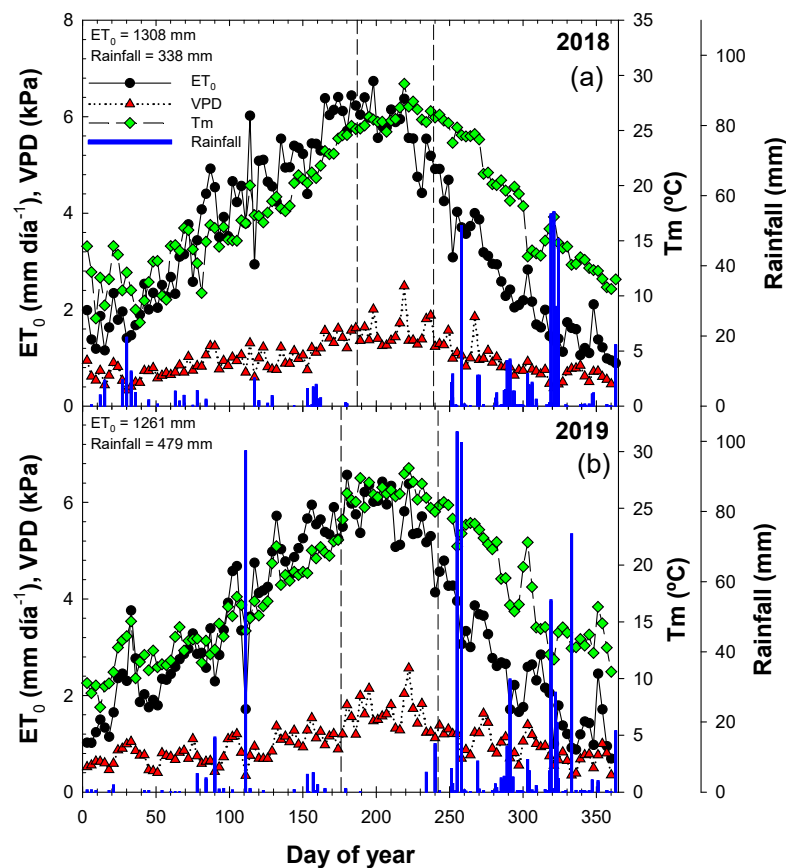


Figure 1. Seasonal evolution of reference evapotranspiration (ET₀), air vapor pressure deficit (VPD), mean air temperature (T_m) and rainfall during the 2018 (a) and 2019 (b) seasons in La Palma (Spain). Broken vertical lines correspond to the beginning of the first drying cycle and the end of the second drying cycle.

2.2. Treatments

All the trees were equally irrigated to maintain field capacity soil water conditions during the irrigation season, except for the two water withholding periods. The experiment was composed of 3 irrigation treatments: (i) control (CTL) trees were irrigated daily to satisfy 115% E_{Tc} during the entire season; (ii) moderate water-stress (MS) trees were subjected to two water withholding cycles until midday stem water potential (Ψ_{stem}) reached -1.3 MPa and -1.7 MPa, first and second cycle, respectively; (iii) severe water-stress (SS) similar to MS, but with different Ψ_{stem} reference values of -1.6 MPa and -2.5 MPa for first and second cycle, respectively. The water withholding periods of both MS and SS trees were followed by recovery irrigation periods which lasted until the water-stress trees reached Ψ_{stem} values similar to the CTL trees. In the first drying cycle, irrigation withdrawal started on 6 July 2018 and 25 June 2019 and was maintained for 12 and 17 days in 2018 and 10 and 21 days in 2019 for MS and SS trees, respectively. The second drying cycle started on 23 July 2018 and 26 July 2019 in MS and on 3 August 2018 and 26 July 2019 in SS trees. The irrigation withdrawal period lasted 15 and 14 days for MS and 24 and 35 days for SS in 2018 and 2019, respectively (Figure 2).

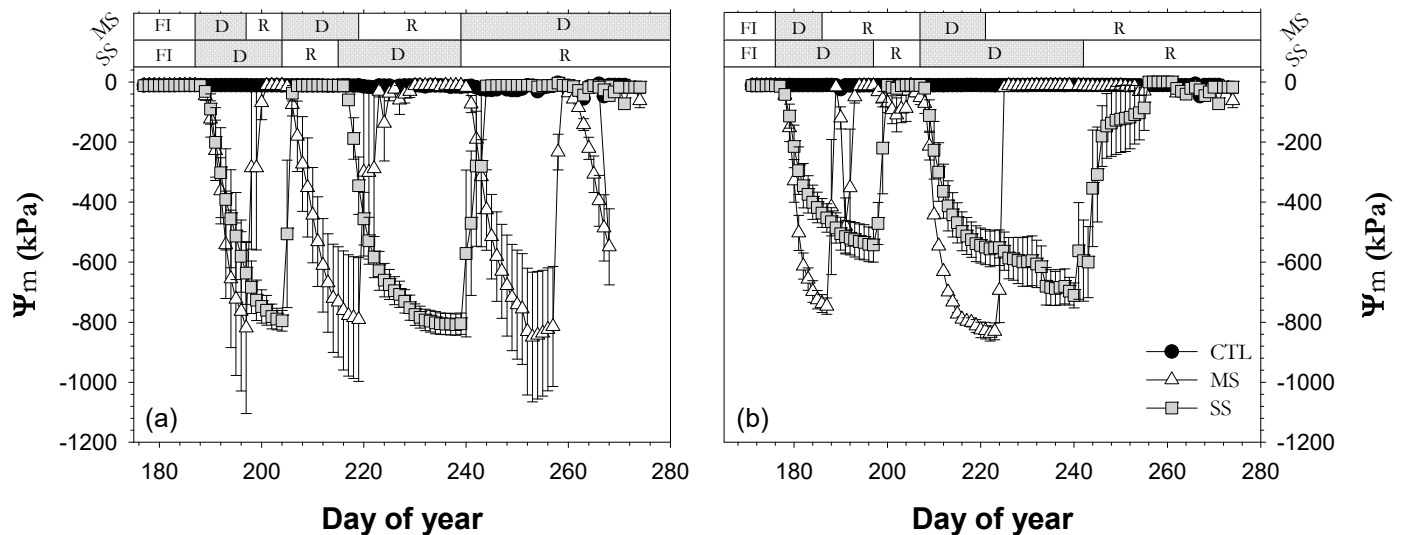


Figure 2. Seasonal evolution of soil matric potential (Ψ_m) at 0.25 m depth in the 2018 (a) and 2019 (b) seasons for the three irrigation treatments: CTL (full irrigation treatment); MS (moderate stress); and SS (severe stress). Each point is the mean \pm SE of 3 sensors per irrigation treatment. FI is full irrigation period, D is drought period, and R is recovery period.

The treatments were distributed according to a completely randomized block design. Each treatment consisted of three replicates, and each replicate had a sampling row of four trees. The measurements were taken in the two central trees per replicate ($n = 6$), with the other trees serving as buffers.

2.3. Field Measurements

2.3.1. Soil Water Status

The soil matric water potential (Ψ_m) was measured with three capacitive sensors with thermal compensation (MPS-6, Decagon Devices, Inc., Pullman, WA, USA) per treatment, at a depth of 25 cm and 15 cm away from the emitter. The Ψ_m values were recorded every 10 min by a datalogger (Model CR1000 with AM16/32B multiplexer, Campbell Scientific Ltd., Logan, UT, USA). The mean Ψ_m value from 06:00 to 08:00 h (solar time), two hours before watering, was calculated and plotted (Figure 2).

2.3.2. Plant Water Status

Predawn leaf water potential (Ψ_{pd} ; just before sunrise), midday leaf water potential (Ψ_{md} ; 11:00 to 13:00 h UT), and Ψ_{stem} were monitored every 3–7 days with a pressure chamber (mod. SF-PRES-70, SolFranc Tecnologías, S.L., Tarragona, Spain), following the recommendations from Turner [27] and Hsiao [28]. Six fully-expanded mature leaves from branches in the lower half of the canopy were selected per treatment to measure Ψ_{pd} and Ψ_{md} . Six healthy, mature, and shaded leaves close to the trunk were used to measure Ψ_{stem} , according to McCutchan and Shackel [29].

Stomatal conductance (g_s) was measured using a CIRAS2 portable gas exchange system (PPSystems, Hitchin, Hertfordshire, UK) at the same time that Ψ_{md} and Ψ_{stem} were measured (11:00 to 13:00 h UT). Six fully-developed leaves per treatment were taken from the middle third of the trees and the sun-exposed side.

To determine whether osmotic adjustment occurred at the end of each water withholding and irrigation recovery period, at predawn and midday, we collected three leaves per replicate close to those used for Ψ_{pd} and Ψ_{md} measurements. The leaves collected at midday were immediately frozen in liquid nitrogen ($-196\text{ }^\circ\text{C}$) and stored at $-40\text{ }^\circ\text{C}$. To determine the osmotic potential at full turgor, the leaves collected at predawn were stored in distilled water overnight at $4\text{ }^\circ\text{C}$ in the dark until they reached full saturation and were then frozen in liquid nitrogen and stored at $-40\text{ }^\circ\text{C}$. Midday leaf osmotic potential (Ψ_o) and leaf osmotic potential at full turgor (Ψ_{os}) were obtained from the stored leaf samples after being thawed at room temperature ($25\text{ }^\circ\text{C}$). Ψ_o was measured with a vapor pressure osmometer (model 5520; Wescor Inc., Logan, UT, USA), according to Gucci et al. [30]. Midday leaf turgor potential (Ψ_{turgor}) was calculated as the difference between midday leaf water and osmotic potentials ($\Psi_{turgor} = \Psi_{md} - \Psi_o$). Similarly, Ψ_{os} was determined on predawn leaves. The active osmotic adjustment was determined as the difference between the Ψ_{os} of stressed and control trees.

2.3.3. Leaf Traits

Every week, four expanded leaves per replicate ($n = 12$) were picked in 2019, and fresh leaf weight (FW) was immediately determined using a scale (AX623, Sartorius AG, Gottingen, Germany), and leaf area (LA) was measured using a leaf-area meter (LI-3100C, LI-COR Inc., Lincoln, NE, USA). The leaves were rehydrated by immersing their petiole in distilled water in the dark at $4\text{ }^\circ\text{C}$ for 18 h to determine leaf weight at full turgor (TW). Subsequently, the leaves were dried to a constant weight in a ventilated oven (Digitheat, JP Selecta SA, Barcelona, Spain) at $70\text{ }^\circ\text{C}$ for 48 h to determine leaf dry weight (DW). Relative water content (RWC, %) was calculated as $RWC = ((FW - DW)/(TW - DW)) * 100$ [31]. The specific leaf weight (SLW, g m^{-2}) was determined as the ratio between DW and LA. Additionally, the leaf dry matter content (LDMC, g g^{-1}) was calculated as the ratio between DW and TW.

2.3.4. Leaf Insertion Angle

The leaf insertion angle (LIA) between the leaf petiole and the stem was determined with a digital protractor (MDA01, Tacklife, New York, NY, USA). Ten random leaves per tree and two trees per replicate ($n = 60$) were measured at 11:00 h (UT). Epinasty (Ep), the change in petiole angle, was calculated as the difference between the LIA of stressed and control trees ($Ep = LIA_{stressed} - LIA_{CTL}$).

2.3.5. Vegetative Growth

Vegetative growth was estimated using the trunk cross-sectional area (TCSA), canopy volume, and pruning wood. At the beginning and the end of each experimental period (at the early of June and at the beginning of October), the trunk diameter was measured with a measuring tape (Pi meter MF612 A, Weiss, Erbendorf, Germany) at 0.15 m above the grafting point in the two central trees per replicate. TCSA was calculated as the circle area from the trunk diameter measured, and the annual increase in trunk cross-sectional area

(Δ TCSA) was calculated as the difference between the TCSA measured at the end and at the beginning of the experiment. In 2019, canopy volume (CV) was calculated before pruning, based on canopy height and diameters (across and within rows) of the two central trees per replicate [32], and the pruning wood weight per tree (PW, kg tree⁻¹) was determined individually during winter dormancy.

2.3.6. Leaf Defoliation

Leaf defoliation was estimated using 3.5 × 2.25 × 0.35 m traps (n = 6). Traps were emptied weekly, and the fallen leaves were dried in a ventilated oven (Digitheat, JP Selecta SA, Barcelona, Spain) at 70 °C until a constant weight was reached. Subsequently, LA and the number of leaves were calculated based on the DW of these leaves. At the end of the study (October), four trees per treatment were covered using anti-bird nets. The leaf area index (LAI) was estimated from the DW and LA measured during the experimental period.

2.4. Statistical Analysis

An analysis of variance (ANOVA) was carried out using the statistical software package Statgraphics centurion XVI (StatPoint Technologies Inc., The Plains, VA, USA) and IBM SPSS Statistic 24 (IBM Corp., Armonk, NY, USA). Post hoc pairwise comparisons between treatments were performed with Duncan's multiple range test at a significance level of 0.05 to determine the significant differences between treatments and variables. A regression analysis was graphed and calculated with SigmaPlot 12.5 (Systat Software Inc., San Jose, CA, USA) and Microsoft Excel (Windows 10 Home, Microsoft Corp., Redmond, WA, USA).

3. Results

3.1. Soil Water Status

The soil matric water potential (Ψ_m) at a depth of 25 cm showed different soil water statuses in the three irrigation treatments due to differential irrigation management (Figure 2). Thus, the drought cycles applied to the MS and SS treatments were clearly defined by Ψ_m . Likewise, the CTL treatment was characterized by constant Ψ_m mean values equivalent to field capacity (≈ -20 kPa) throughout the irrigation season. Moderate (MS) and severe (SS) drought-stress treatments showed Ψ_m values similar to CTL during the pre-drought period and in most of the recovery periods. During the non-irrigation periods, however, Ψ_m rapidly decreased in both stress treatments and stabilized at around -840 kPa (2018), with slightly higher values (less negative) found for SS in 2019. In general, Ψ_m recovered quickly after the restart of irrigation, except for the second drought cycle in 2019. Moreover, despite the longer duration of the drought periods in the SS treatment, the MS treatment obtained lower Ψ_m minimum values than those of SS in both drought cycles in 2019.

3.2. Plant Water Status

Ψ_m , Ψ_{pd} , Ψ_{md} , and Ψ_{stem} characterized the sequence of drought-irrigation cycles in the MS and SS conditions. The Ψ_{pd} , Ψ_{md} , and Ψ_{stem} mean values were -0.32 , -1.74 and -0.65 MPa, respectively, in CTL trees (Figure 3). These values were constant throughout the experimental period, and they were typical of well-watered trees. Ψ_{md} showed greater variability than Ψ_{pd} and Ψ_{stem} , as they were more influenced by the current weather conditions (Figure 1). Before withholding irrigation, the MS and SS trees showed values similar to those of CTL trees. However, when irrigation was withheld, the values of the three water potential plant indicators gradually decreased in MS and SS trees. The minimum values of leaf water potential were lower in the second drought cycle than in the first one, as forecasted. The Ψ_{pd} , Ψ_{md} , and Ψ_{stem} minimum mean values reached at the end of the first and second drought periods in MS versus SS trees were -0.6 and -1.0 MPa vs. -0.9 and -1.4 MPa (Ψ_{pd}), -2.2 and -2.8 MPa vs. -2.5 and -3.1 MPa (Ψ_{md}), and -1.3 and -1.8 MPa vs. -1.7 and -2.3 MPa (Ψ_{stem}) for the study period. In

general, the slope of Ψ_{md} was steeper in the second cycle than in the first cycle. After both drought cycles, during the recovery periods with irrigation at 115% ET_c , the MS and SS trees reached Ψ_{md} values similar to CTL trees. The duration of each recovery period was dependent on the intensity of water stress reached. In 2018, even though a third water-withholding period in the MS treatment had been started, it could not be completed due to the rainfalls in September (Figure 1).

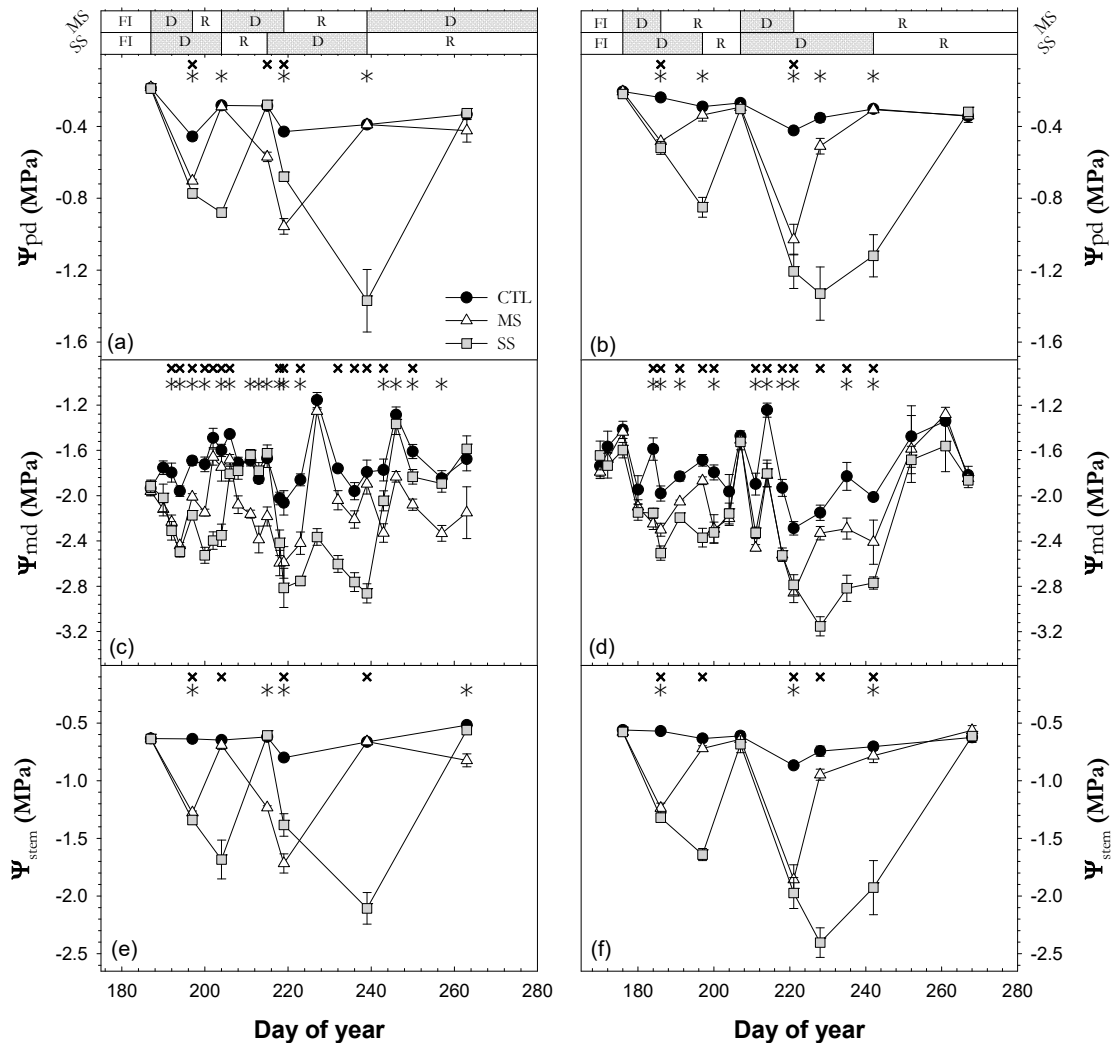


Figure 3. Seasonal evolution of (a,b) predawn leaf water potential (Ψ_{pd}), (c,d) midday leaf water potential (Ψ_{md}), and (e,f) midday stem water potential (Ψ_{stem}) during the 2018 (a,c,e) and 2019 (b,d,f) seasons for the three irrigation treatments: CTL (full irrigation treatment); MS (moderate stress treatment); and SS (severe stress treatment). Each point is the mean \pm SE of 6 leaves per treatment. Asterisks and crosses indicate statistically significant differences between CTL and MS and CTL and SS, respectively, according to Duncan’s multiple range test ($p < 0.05$). FI, D, and R are full irrigation, drought, and recovery periods, respectively.

The relationships between Ψ_{pd} vs. Ψ_{md} and Ψ_{pd} vs. Ψ_{stem} were examined via a linear correlation analysis (Figure 4). All three indicators were highly correlated with one another. Ψ_{pd} was more strongly related to Ψ_{stem} than Ψ_{md} , although both relationships showed a high coefficient of determination ($R^2 = 0.94^{***}$ for Ψ_{stem} and $R^2 = 0.85^{***}$ for Ψ_{md}).

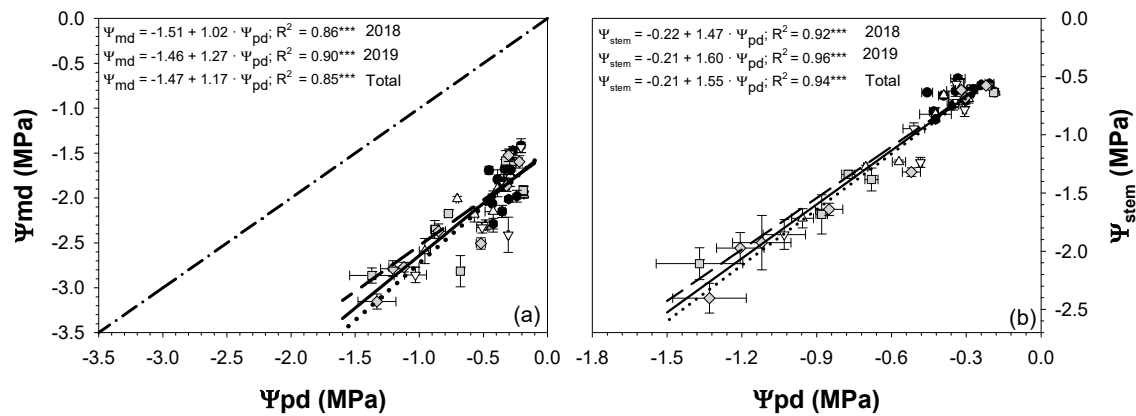


Figure 4. Linear relationships between predawn leaf water potential (Ψ_{pd}) and midday leaf water potential (Ψ_{md}) (a) and midday stem water potential (Ψ_{stem}) (b) in the 2018 and 2019 seasons for the three irrigation treatments: CTL (full irrigation treatment; 2018: ●; 2019: ●); MS (moderate stress; 2018: △; 2019: ▽); and SS (severe stress; 2018: ■; 2019: ◆). Each point is the mean \pm SE of 6 trees per treatment. *** correspond to p -values ≤ 0.001 .

Stomatal conductance (g_s) decreased due to water stress. While the CTL trees maintained g_s values above $315 \text{ mmol m}^{-2} \text{ s}^{-1}$, the MS and SS trees reduced their values by 45 and 55% at the end of the first drought cycle and 55 and 73% at the end of the second drought, as compared with CTL trees. The g_s values were similar to CTL trees during the pre-drought period (Table 1).

Table 1. Mean values for stomatal conductance ($\text{mmol m}^{-2} \text{ s}^{-1}$) of the three irrigation treatments: CTL (full irrigation treatment), MS (moderate stress), and SS (severe stress) in the 2019 season.

Period	DOY	Treatment		DOY	Treatment	
		CTL	MS		CTL	SS
Full irrigation	176	364.8 ± 40.8 a	404.8 ± 23.4 a	176	364.8 ± 40.8 a	369.3 ± 23.3 a
First drought cycle	186	416.3 ± 49.7 a	228.8 ± 41.7 b	197	401.3 ± 58.4 a	180.5 ± 14.3 b
First recovery cycle	207	350.3 ± 18.3 a	365.7 ± 9.7 a	207	350.3 ± 18.3 a	346.3 ± 15.8 a
Mid-second drought cycle	-	-	-	228	371.3 ± 27.3 a	103.2 ± 6.7 b
Second drought cycle	221	316.0 ± 13.7 a	123.7 ± 16.8 b	242	364.3 ± 37.5 a	100.2 ± 13.5 b
Second recovery cycle	242	364.3 ± 37.47 a	351.7 ± 11.89 a	268	347.7 ± 3.7 a	329.5 ± 22.4 a

Mean values followed by different letters in the same row indicate significant differences between treatments based on ANOVA ($p < 0.05$).

For the CTL trees, the midday leaf osmotic potential (Ψ_o) values ranged from -2.46 to -2.94 MPa, with the highest values at the end of September, although the most common values were around -2.85 and -2.67 MPa in 2018 and 2019, respectively. Overall, there were no significant differences between the drought treatments and CTL values in 2018. The only exceptions were at the end of August 2018 between SS ($\Psi_o = -3.14$ MPa, 239 DOY) and CTL trees and in mid-August 2019 between the stress treatments and the CTL trees.

The average midday leaf turgor potential (Ψ_{turgor}) of the CTL trees was higher in 2018 (1.0 MPa) than in 2019 (0.8 MPa). The Ψ_{turgor} of the MS and SS trees had a greater relative variation with respect to CTL than Ψ_o . Generally, the MS and SS trees had significantly lower Ψ_{turgor} values than CTL trees (Figure 5). Once the drought period started, Ψ_{turgor} decreased, reaching its lowest values in SS trees as expected. The lowest Ψ_{turgor} values were reached in the second drought cycle, being very similar for each treatment in both years ($\Psi_{turgor} = 0.32$ MPa in MS and practically 0.0 MPa in SS, i.e., total loss of turgor). The longer duration of the drying cycles in the SS trees as compared with the MS trees resulted in the stabilization of the lowest values, especially in the second drought cycle. This was not observed in the MS trees. After restarting irrigation at 115% of the ETc, both deficit

treatments reached Ψ_{turgor} values similar to those of the CTL trees (Figure 5). Ψ_{md} showed a stronger linear relationship with Ψ_{turgor} ($R^2 = 0.85$; Figure 6a) than with Ψ_o (Figure 6b). Moreover, it was observed that the Ψ_o values measured were similar (line 1:1) to those of Ψ_{md} when Ψ_{md} values were below -3.0 MPa (Figure 6b), due to Ψ_{turgor} values being closer to 0 MPa (leaf turgor point loss).

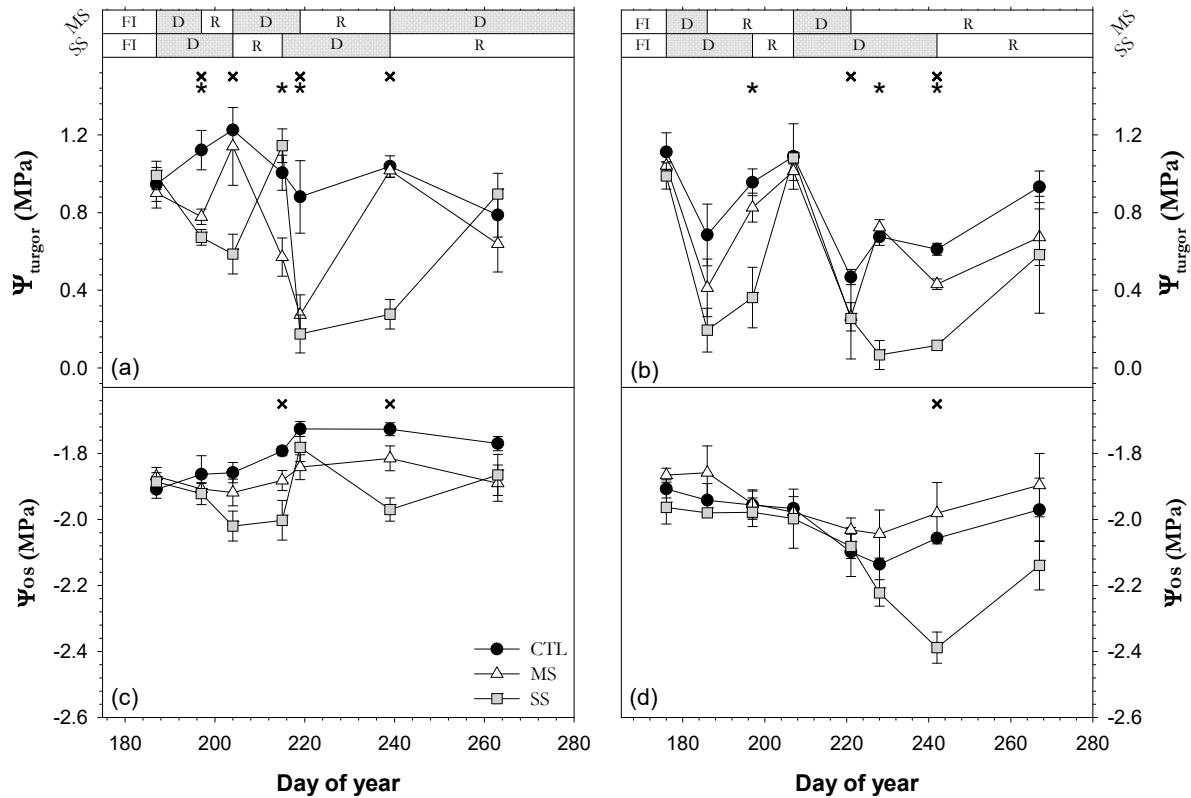


Figure 5. Seasonal evolution of (a,b) midday leaf turgor potential (Ψ_{turgor}) and (c,d) predawn leaf osmotic potential at full turgor (Ψ_{os}) in the 2018 (a,c) and 2019 (b,d) seasons for the three irrigation treatments: CTL (full irrigation treatment); MS (moderate stress); and SS (severe stress). Each point is the mean \pm SE of 9 leaves per treatment. Asterisks and crosses indicate significant differences between CTL and MS and CTL and SS, respectively, according to Duncan’s multiple range test ($p < 0.05$). FI is full irrigation period, D is drought period, and R is recovery period.

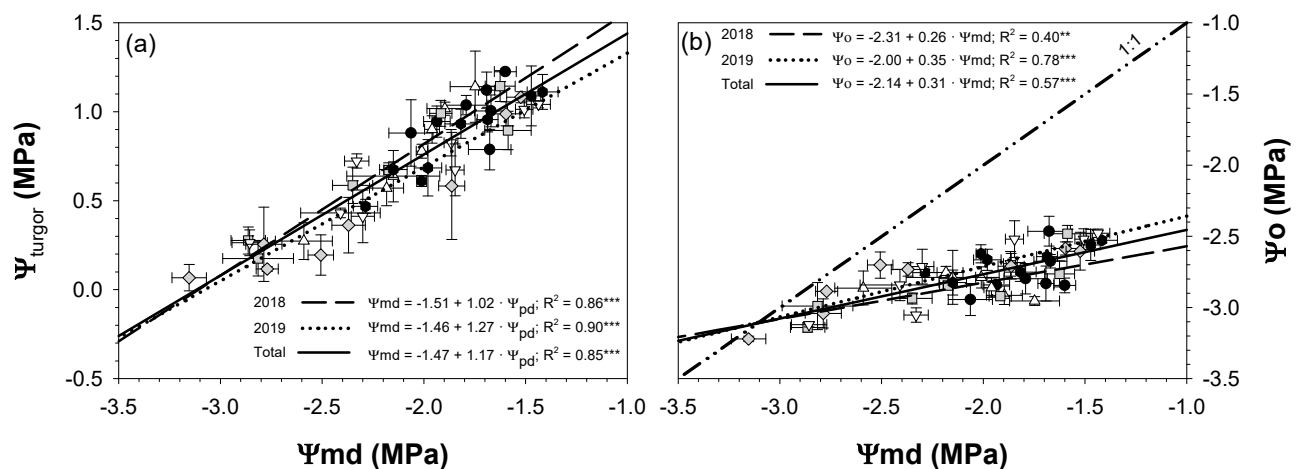


Figure 6. Linear relationships between leaf turgor potential (Ψ_{turgor}) and midday leaf water potential (Ψ_{md}) (a); and between midday leaf osmotic potential (Ψ_o) and Ψ_{md} (b) in the 2018 and 2019 seasons for the three irrigation treatments CTL (full irrigation treatment; 2018: ●; 2019: ●); MS (moderate stress; 2018: △; 2019: ▽); and SS (severe stress; 2018: ■; 2019: ◇). Each point is the mean \pm SE of 6 trees per treatment. ** and *** correspond to p -values ≤ 0.01 and 0.001 .

The mean values of predawn leaf osmotic potential at full turgor (Ψ_{os}) of the CTL trees were -1.8 and -2.0 MPa in 2018 and 2019, respectively (Figure 5c,d). We did not find significant differences in Ψ_{os} between MS and CTL trees in any year of study. However, we observed some significant differences in Ψ_{os} between SS and CTL trees in both years after the second drought period (early and late August 2018 and late August 2019). While in 2018, the Ψ_{os} values showed a pattern in accordance with the water regime applied, in 2019, the MS values tended to be higher than those of CTL. An osmotic adjustment was observed on three different days during the study period (two in 2018 and one in 2019) but only in SS plants and on the last day of each drought period. The maximum osmotic adjustment reached was -0.4 MPa (DOY 242 in 2019). This osmotic adjustment was not able to maintain positive Ψ_{turgor} values in any stress treatment or year of study (Figure 5a,b).

3.3. Leaf Traits

Drought stress did not affect specific leaf weight (SLW) or leaf dry matter content (LDMC). However, we observed increasing SLW (from 84.5 to 97.5 g m^{-2}) and LDMC (from 0.29 to 0.35 g g^{-1}) trends as the season progressed (Figure 7a,b) and the age of the leaf increased. In contrast, RWC remained relatively constant in CTL trees, while in MS and SS trees, it decreased with the onset of the drought periods. This RWC decrease was clearer in SS trees, particularly in the second drought cycle, as expected. Significant differences were observed in RWC between irrigation treatments during the first drought cycle in 2019 but not in the second cycle due to the higher variability of the measurements. (Figure 7c).

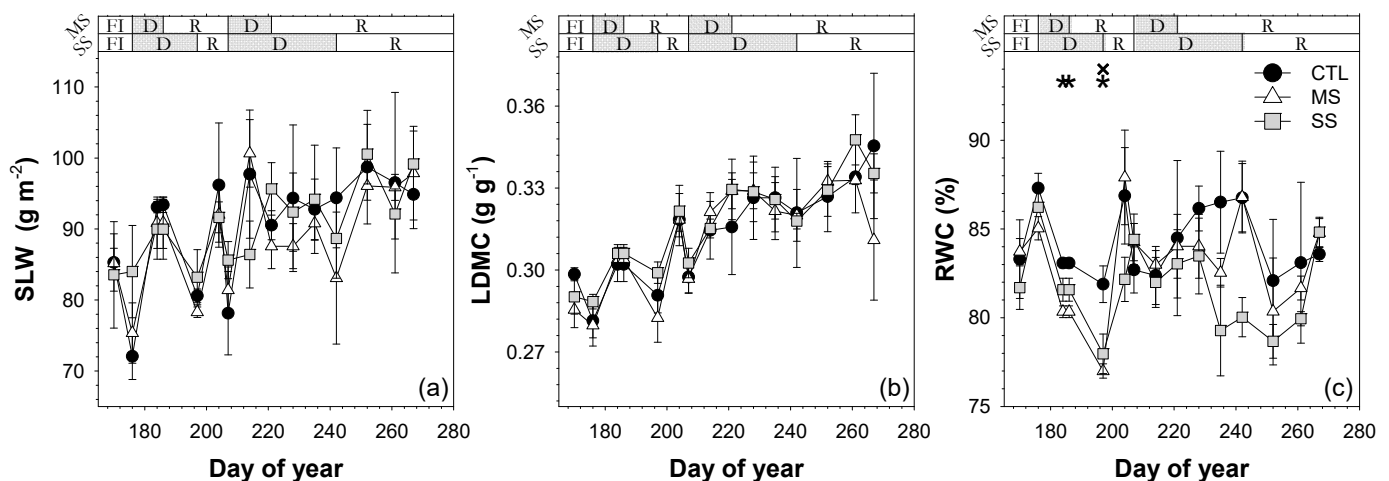


Figure 7. Seasonal evolution of (a) specific leaf weight (b), leaf dry-matter content and (c) relative water content in the 2019 season for the three irrigation treatments: CTL (full irrigation treatment); MS (moderate stress); and SS (severe stress). Each point is the mean \pm SE of 12 leaves per treatment. Asterisks and crosses indicate significant differences between CTL and MS and CTL and SS, respectively, according to Duncan's multiple range test ($p < 0.05$). FI is the full irrigation period, D is the drought period, and R is the recovery period.

3.4. Leaf Insertion Angle

The irrigation treatment affected the leaf insertion angle (LIA; Figure 8). Water stress caused a gradual increase in LIA in both years of study. Thus, in the drought periods, MS and SS leaves showed values higher than those of CTL trees. CTL trees maintained relatively constant LIA values during the experimental period. Maximum values of epinasty were 32.1° (DOY 239 in 2018) and 23.6° (DOY 228 in 2019) for MS and SS, respectively (Figure 8).

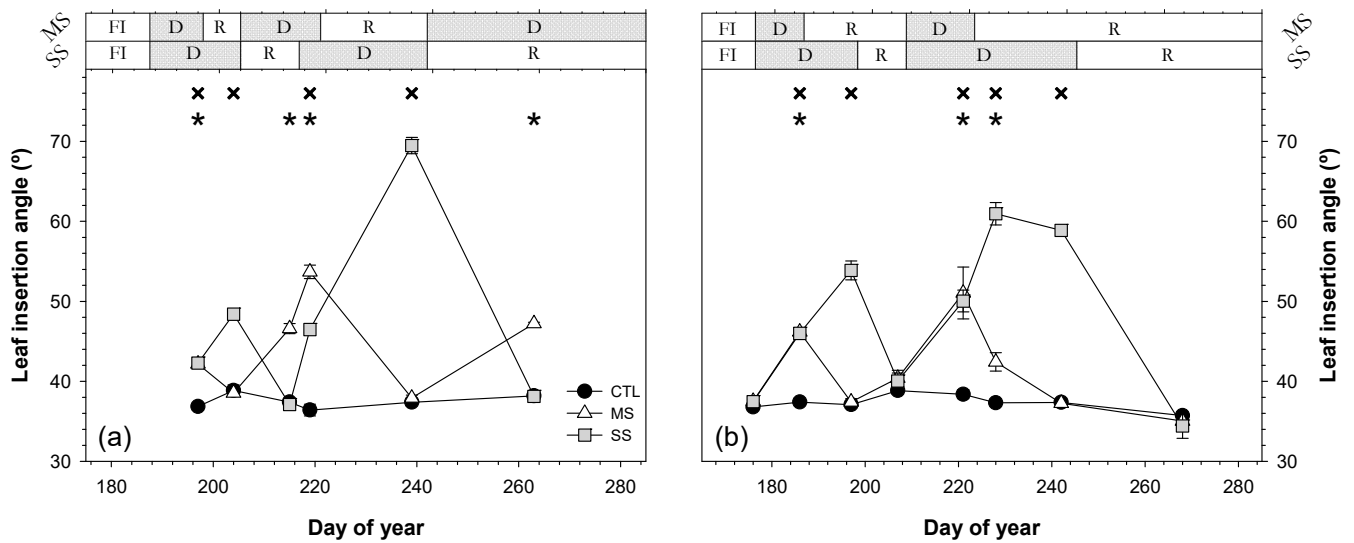


Figure 8. Seasonal evolution of leaf insertion angle during the 2018 (a) and 2019 (b) seasons for the three irrigation treatments: CTL (full irrigation treatment); MS (moderate stress); and SS (severe stress). Each point is the mean \pm ES of 60 leaves per treatment. Asterisks and crosses indicate statistically significant differences between CTL and MS and CTL and SS, respectively, according to Duncan’s multiple range test ($p < 0.05$). FI is full irrigation period, D is drought period, and R is recovery period.

Figure 9 shows the linear relationships between LIA and Ψ_{stem} . The figure illustrates the dependence of LIA on the plant water status. The range of LIA values under the experimental conditions ranged from 35° to 70° . The value of 35° corresponded to conditions of well-irrigated trees (CTL treatment), while 70° was observed under severe plant water stress deficit (SS treatment; Figure 3). LIA exhibited a strong linear relationship with Ψ_{stem} ($R^2 = 0.85$ ***).

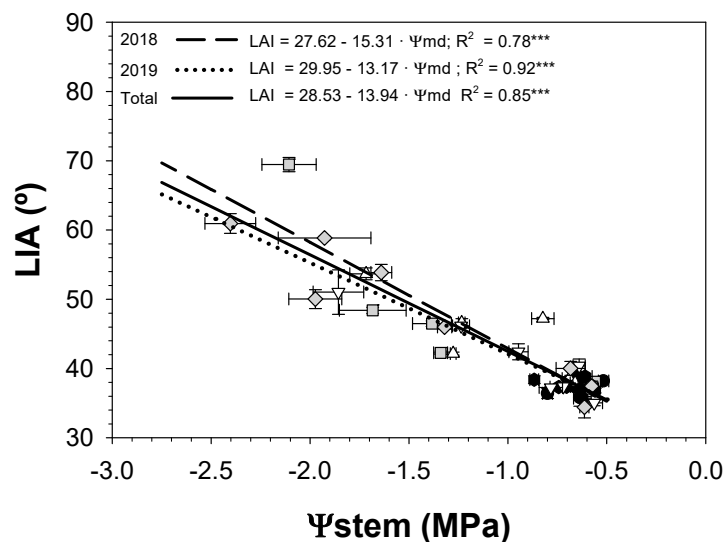


Figure 9. Relationship between midday stem water potential (Ψ_{stem}) and leaf insertion angle (LIA) in the 2018 and 2019 seasons for the three irrigation treatments: CTL (full irrigation treatment; 2018: ●; 2019: ●); MS (moderate stress; 2018: △; 2019: ▽); and SS (severe stress; 2018: □; 2019: ◇). Each point is the mean \pm SE of 6 trees per treatment. *** correspond to p -values ≤ 0.001 .

3.5. Vegetative Growth

Vegetative growth was assessed through the trunk cross-sectional area (TCSA), canopy volume (CV), and pruning wood weight (PW; Table 2). In general, vegetative growth was sensitive to water deficit, and significant differences were found among treatments. Although TCSA was similar in all the treatments at the beginning and end of 2018, the increase in TCSA (Δ TCSA) resulted in significant differences (Table 2). Conversely, we observed significant differences in TCSA at the end of 2019 after two irrigation seasons. Consequently, Δ TCSA decreased as a result of water deficit in both years of study. The CTL trees experienced greater growth than MS and SS trees as the experiment progressed. The average Δ TCSA values in CTL trees were 6.65 and 12.31 cm² against 4.88 and 6.86 cm² for SS trees in 2018 and 2019, respectively. Similarly, the CV and PW of MS and SS trees were lower than those of CTL trees, while no differences were observed in these growth variables between MS and SS trees. On a percent basis, the overall reduction in CV with respect to CTL trees was 37.87 and 63.83% for MS and SS trees, respectively.

Table 2. Influence of the three irrigation treatments, control (CTL), moderate-stress water (MS), and severe-stress water (SS), on the vegetative growth of ‘Lapins’ sweet cherry trees over the 2018 and 2019 seasons.

	Variable		Year	CTL	MS	SS
TCSA	cm ²	Initial	2018	19.29 ± 2.11 a	20.52 ± 1.79 a	19.90 ± 1.50 a
TCSA	cm ²	End	2018	25.94 ± 2.15 a	25.66 ± 1.86 a	24.78 ± 1.62 a
Δ TCSA	cm ²	-	2018	6.65 ± 0.21 a	5.15 ± 0.13 b	4.88 ± 0.12 b
TCSA	cm ²	Initial	2019	27.59 ± 2.42 a	29.67 ± 0.42 a	26.71 ± 1.51 a
TCSA	cm ²	End	2019	39.90 ± 3.39 a	38.94 ± 0.55 a	33.57 ± 2.07 b
Δ TCSA	cm ²	-	2019	12.31 ± 0.98 a	9.27 ± 0.41 b	6.86 ± 0.57 c
CV	m ³ tree ⁻¹	Initial	2019	1.10 ± 0.15 a	1.03 ± 0.17 a	0.94 ± 0.13 a
CV	m ³ tree ⁻¹	End	2019	2.30 ± 0.16 a	1.25 ± 0.18 b	1.16 ± 0.12 b
Δ CV	m ³ tree ⁻¹	-	2019	1.20 ± 0.17 a	0.38 ± 0.12 b	0.22 ± 0.02 b
PW	kg tree ⁻¹	-	2019	2.35 ± 0.44 a	1.46 ± 0.48 ab	0.85 ± 0.25 b

TCSA—trunk cross-sectional area; CV—canopy volume; PW—pruning wood. Mean values ± ES (n = 6) followed by different letters within the same column denote significant differences according to Duncan multiple range test ($p < 0.05$).

3.6. Leaf Defoliation

The number of fallen leaves was highly sensitive to drought stress (Figure 10). According to the 2019 data, the intensity of water stress suffered by the MS trees was not enough to generate significant differences with the CTL trees regarding the fallen leaves. In contrast, SS trees showed fallen leaves dry weight (FLDW) and fallen leaves area (FLA) that were significantly higher than CTL and MS trees (Figure 10).

During the first drought cycle in the SS treatment, water stress did not increase the amount of fallen leaves from SS trees. However, during the second drought cycle, the fallen leaves value of the SS trees was much higher than in the CTL and MS trees (Figure 10). The first significant difference in FLDW was observed when Ψ_{stem} dropped below -2.0 MPa (Figure 3c). The fact that CTL trees had satisfied their full crop water requirements during the 2018 and 2019 growing seasons resulted in trees with a significantly higher number of leaves and consequently a higher leaf area index, LAI, than MS and SS trees (Table 3).

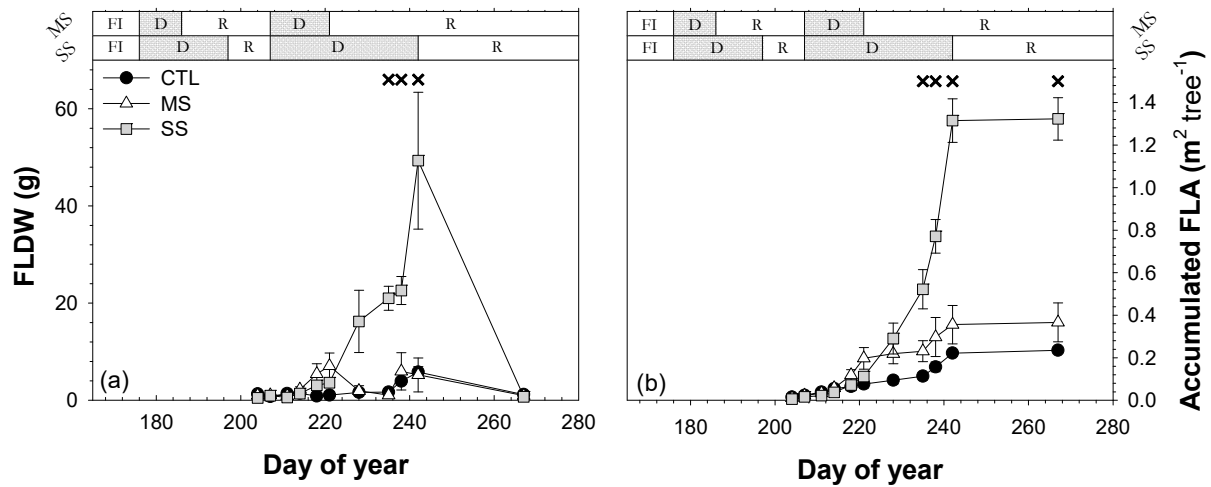


Figure 10. Seasonal evolution of (a) fallen leaves dry weight (FLDW) and (b) Accumulated fallen leaves area (FLA) in the 2019 season for the three irrigation treatments: CTL (full irrigation treatment); MS (moderate stress); and SS (severe stress). Each point is the mean \pm ES of 6 trees per treatment. Asterisks and crosses indicate statistically significant differences between CTL and MS and CTL and SS, respectively, according to Duncan’s multiple range test ($p < 0.05$). FI is full irrigation period, D is drought period, and R is recovery period.

Table 3. Effect of drought stress on number of leaves per tree, total leaf area, and leaf area index (LAI) for the three irrigation treatments at the end of 2019.

Variable	CTL	MS	SS
Number of leaves per tree	1611.75 \pm 83.74 a	735.02 \pm 80.94 b	682.57 \pm 172.55 b
Total leaf area (m ² tree ⁻¹)	11.33 \pm 0.59 a	5.17 \pm 0.57 b	4.74 \pm 1.20 b
LAI (m ² m ⁻²)	1.44 \pm 0.07 a	0.66 \pm 0.07 b	0.60 \pm 0.15 b

LAI—leaf area index. Mean values \pm ES (n = 4) followed by different letters within the same column denote significant differences according to Duncan multiple range test ($p < 0.05$).

4. Discussion

One of the earliest physiological responses of ‘Lapins’ sweet cherry trees to both moderate and severe irrigation withholding was a reduction in plant water potentials, Ψ (Ψ_{pd} , Ψ_{md} , and Ψ_{stem} ; Figure 3). The irrigation withholding led to lower Ψ_m mean values in the MS and SS treatments than the CTL treatment during the drought periods, which took place in the dry summer months (Figure 1). The fast decrease in leaf water potential could indicate that the soil water reservoir was insufficient for slowing down the decrease in Ψ (Figure 3). This was most likely due to low water reserves in the not-wetted area at that time, which were unable to alleviate the decrease in the soil water content of the wetted area during the drought cycles. The relative stabilization of Ψ_m to around -840 kPa (Figure 2) could be the result of the strong water retention by soil micropores and a high reduction in the rate of transpiration. This reduction in transpiration would be caused by both efficient stomatal regulation and leaf shedding (Table 1 and Figure 10) [33]. The influence of Ψ_m on plant water status was reflected in the evolution of Ψ_m and Ψ (Figures 2 and 3). Thus, plant water status decreased progressively as Ψ_m decreased during periods of drought. MS and SS reached post-harvest Ψ_m mean values below -200 and -300 kPa, which is indicative of the level of water deficit reached, as they included recovery periods.

The Ψ_{stem} values of the CTL trees were above -0.75 MPa, except for one measurement in 2019 (Figure 3c). These values indicated an adequate water supply to satisfy the full crop water requirements [34]. However, the MS and SS trees occasionally reached Ψ_{stem} values of -1.85 and -2.40 MPa, respectively. These values are clearly indicative of water stress conditions [10]. Marsal et al. [34] pointed out that incipient leaf wilting in cherry trees can be observed in the field at a Ψ_{stem} of -1.80 MPa. Taking into consideration these

Ψ_{stem} values, it could be stated that MS and SS trees suffered moderately severe and severe stress, respectively.

The behavior followed by the seasonal patterns of Ψ_{stem} and Ψ_{pd} during the withholding and resuming irrigation periods was very similar (Figure 3). Furthermore, the linear relationship between Ψ_{pd} and Ψ_{stem} ($R^2 = 0.94$ ***; Figure 4b) was stronger than Ψ_{pd} vs Ψ_{md} ($R^2 = 0.85$ ***; Figure 4a). This is in agreement with the findings from different authors, in that Ψ_{pd} and Ψ_{stem} were better and more useful indicators of plant water status than Ψ_{md} [35,36]. It should be noted that Ψ_{md} was more influenced by current weather conditions than Ψ_{pd} and Ψ_{stem} . The fact that Ψ_{pd} was measured at predawn and Ψ_{stem} used covered leaves close to the trunk resulted in smaller variability than Ψ_{md} by disrupting leaf transpiration. The slope of the linear relationship Ψ_{pd} vs. Ψ_{md} for both years was higher than unity (slope = 1.17; Figure 4a), suggesting the extremely anisohydric character of sweet cherry trees [37].

MS and SS trees required 7–14 days to reach Ψ_{stem} values that were similar to those of the CTL trees after each withholding irrigation period (Figure 3). The length of the first and second recovery periods was dependent on the timing, duration, and intensity of the water stress reached. Fereres et al. [38] observed a similar recovery period in an experimental study with mature orange trees. Conversely, different studies in pots [15,18] reported a quicker recovery, two days or earlier, after restarting irrigation. This could be due to the different growing conditions between trees in pots and trees under field conditions. These differences include a faster recharge of the soil water stock and a higher percentage of wetted soil in pots than in the ground, among others.

When sweet cherry trees were subjected to soil drying cycles lasting about 10–15 days and 20–30 days during the first and second cycles, respectively, Ψ_{md} decreased about 0.30 MPa and 0.75 MPa with respect to CTL trees during the first and second drying cycle (Figure 3), depending on the length of the drying cycle. Around 95% of this change was explained by a decrease in Ψ_{turgor} in 2018, while in 2019, this was 40–85%. Both of these results could result from dehydration processes (Figure 7c), which promoted wilting plant symptoms (Figure 10 and Table 3) without becoming permanent wilting. Likewise, Castel and Fereres [14] and Conesa et al. [39] reported that water stress caused a decrease in Ψ_{turgor} values close to zero in almond trees and table grapes subjected to drying cycles and sustained deficit irrigation, respectively. Contrary to Ψ_{md} and Ψ_{turgor} , Ψ_{os} remained practically constant during the entire study period in the MS and SS trees, except at the end of both second drying cycles, when Ψ_{os} decreased significantly in SS trees (Figure 5). This significant difference in Ψ_{os} was preceded by a progressive but slow decrease in Ψ_{os} in SS trees, which suggests that the ability of sweet cherry trees to perform osmotic adjustment (OA) was limited (c. 0.3 MPa), requiring the high water stress level to be achieved progressively. Although OA was unable to maintain Ψ_{turgor} values at a level similar to those of the CTL trees, these Ψ_{turgor} values were above zero (Figure 5). A similar response was reported in peach trees by Mellisho et al. [40]. Castel and Fereres [14] reported that the OA capacity of young almond trees under water stress was limited, establishing their capacity for OA at around 0.3 MPa. However, according to Turner [22], in practice, partial turgor maintenance is more common than full turgor, as the accumulation of solutes is not enough to fully compensate for the reduction in water potential, and consequently, the turgor decreases, but to a lesser extent than if no solute accumulation occurred.

Stomatal conductance clearly decreased during the drought cycles, with values equivalent to 55 and 45% of the CTL trees in the first drying cycle and 45 and 27% in the second drying cycle for MS and SS trees, respectively (Table 1). Similar behaviors were found by Mellisho et al. [40] in peach trees and Bhusal et al. [41] in *Prunus sargentii*. A partial closure of the stomata would help to maintain a certain level of cell turgor, which would allow for the development of turgor-dependent processes and drought avoidance [42]. At the end of the recovery periods, both MS and SS trees showed similar g_s values to those of the CTL trees, thereby showing the full functionality of the stomata. A strategy followed in apricot

trees is to delay or regulate the stomata opening after resuming irrigation, which allows them to reach full turgor of the cells faster [15].

The seasonal patterns of SLW and LDMC were similar for all the trees from the three irrigation treatments (Figure 7). Consequently, there was no increase in the density or thickness of foliar tissue caused by drought stress [43]. This is consistent with the generality of Ψ_{os} values obtained, as we only observed significant differences in Ψ_{os} between the trees from the extremely different CTL and SS treatments once in 2019 and twice in 2018 (Figure 5). The accumulation of osmolytes was not sufficient for it to have an influence on SLW and LDMC traits and to maintain high Ψ_{turgor} values (Figure 5a). Egea et al. [44] reported that the increases in SLW throughout the season could be motivated by intrinsic characteristics of the species rather than by water stress intensity alone, which could be extended to LDMC. It is clear that *P. sargentii* increased the SLW under heavy drought to reduce the leaf size, which is advantageous, as it could reduce canopy temperature and improve water use efficiency [41]. The RWC values of MS and SS leaves decreased during the drying cycles as a result of dehydration of the cells, which could have contributed to a relative change in cell volume of leaf tissues [45] and to the maintenance or even decrease in the Ψ_o values through lower hydration levels [46]. The fact that g_s was equal or greater than $100 \text{ mmol m}^{-2} \text{ s}^{-1}$ at the most critical moments of the SS strategy (Table 1) supports the evidence that SS leaves did not reach the lower limit of RWC, where tree regulation is deficient, and metabolism is unable to maintain vital functions [47].

The angle between the leaf petiole and the stem where it is attached increased during the water withholding periods (Figure 8) as a result of transpiration (Table 1) and loss of turgor pressure (Figure 5). Our results support the turgor-dependent nature of the LIA [48] in sweet cherry trees (Figure 9). It is well known that a change in LIA is a water conservation mechanism, which allows the reduction in the incident solar radiation and, therefore, the minimization of water loss and leaf heating [15]. Briglia et al. [49] obtained similar LIA responses in grapevines as those obtained in our experiment on sweet cherry trees. They observed a variation in LIA from 75° (well-irrigated plants) to 110° (severe drought stress) and a linear increase in LIA in response to decreasing of Ψ_{stem} . However, the epinasty values recorded in our study on sweet cherry trees were relatively higher than those observed in grapevines [49], given the increase from 35° on well-irrigated trees to 70° in SS trees. The recovery of epinasty in both water deficit treatments occurred at the end of each recovery period. LIA was full and reversible (Figure 8) once the irrigation resumed, although LIA recovery could vary depending on rehydration type and species [50]. The leaf petiole angle in sweet cherry trees was positively correlated with Ψ_{stem} (Figure 9). For this reason, LIA may be used as a rapid and simple morphological parameter to predict the plant water status of sweet cherry trees.

The MS and SS trees showed a lower vegetative growth than well-watered trees (CTL). Water stress reduced $\Delta TCSA$ by 24% and 38% for the MS and SS trees, respectively, during the 2018–2019 period (Table 2). The effect of drought stress was more evident at the end of 2019 than in 2018 as a consequence of the accumulated response to the water deficit. Just as $\Delta TCSA$, canopy volume (CV) and pruning wood (PW) decreased due to the effect of the drought stress, from 68% (MS) to 82% (SS) and from 38% (MS) to 64% (SS) with respect to the CTL trees in 2019 (Table 2), coinciding with the results reported in ‘Brooks’ sweet cherry trees by Livellara et al. [21]. The lowest growth in CV and PW could be due to smaller shoot lengths under irrigation withholding cycles [10]. The influence of water stress on vegetative parameters is widely known, as water is one of the strongest factors which affect vegetative growth [41,44] and cell expansion [51] in plants. Moreover, prolonged water stress on vegetative growth could result in a reduction in photosynthesis [41] and lower carbohydrate accumulation, which could reduce the plant’s reserves [52] and negatively affect vegetative growth in the following years, which is a key factor in determining the following year’s yields. Severe water stress ($\Psi_{stem} < -2.0 \text{ MPa}$) not only resulted in a significant reduction in vegetative growth. It also caused premature defoliation (Figure 10) as a further step in water conservation to that promoted by epinasty. In SS trees, defoliation

was an important adaptive mechanism for drought tolerance (Table 3), as it clearly reduced the leaf area of the trees and thus the area exposed to solar radiation [53]. In SS trees, the decrease in Ψ_{turgor} at the end of the second drought cycle coincided with the moment in which they shed the highest number of leaves, while in MS trees, there was a low amount of leaf fall, which was more similar to CTL trees (Figures 5 and 10). This implies that it is necessary to reach Ψ_{turgor} values close to the turgor loss point (0 MPa) to promote significant amounts of leaf drop.

5. Conclusions

The above-mentioned results can contribute to more complete knowledge of drought-adaptive mechanisms in young sweet cherry trees. Sweet cherry trees mainly showed avoidance strategies to drought stress. Thus, the trees subjected to water deficit were unable to develop a leaf osmotic adjustment that could maintain high turgor pressure and plant hydration at levels similar to control trees. Leaf turgor loss decreased the tree's vegetative growth and increased the leaf insertion angle as a mechanism to reduce the incident solar radiation. At the end of the drought periods, leaf turgor loss led to significant stomatal closure, reducing water loss by transpiration in sweet cherry trees exposed to water stress. If drought stress persists ($\Psi_{\text{stem}} < -2.0$ MPa), then the above mechanisms, combined with a significant reduction in leaf area through defoliation, could have a significant impact in the following years or lead to total plant collapse. It is therefore recommended to maintain a stem water potential above -2.0 MPa during post-harvest in sweet cherry orchards managed under regulated deficit irrigation.

The strong relationship between leaf insertion angle and plant water potentials in sweet cherry trees could constitute a new research line. Thus, machine-based monitoring composed of camera devices with integrated processing systems could be used to determine the plant water status from changes in leaf insertion angles.

Author Contributions: Conceptualization, P.J.B.-R., V.B. and R.D.; methodology, P.J.B.-R., V.B. and R.D.; software, P.J.B.-R. and R.T.-S.; validation, V.B., P.J.B.-R. and R.D.; formal analysis, P.J.B.-R. and V.B.; investigation, P.J.B.-R., V.B., R.T.-S. and R.D.; resources, R.T.-S. and R.D.; data curation, P.J.B.-R. and R.D.; writing—original draft preparation, P.J.B.-R., V.B. and R.D.; writing—review and editing, V.B., R.D. and R.T.-S.; visualization, P.J.B.-R. and V.B.; supervision, P.J.B.-R., V.B., R.D. and R.T.-S.; project administration, R.D. and R.T.-S.; funding acquisition, R.D. and R.T.-S. All authors have read and agreed to the published version of the manuscript.

Funding: This research was funded by the Spanish Economy and Competitiveness Ministry (MINECO) and the European Agricultural Funds for Rural Development. References: AGL2013-49047-C2-1-R, AGL2016-77282-C33-R and PID2019-106226RB-C22/AEI/10.13039/501100011033. Pedro José Blaya-Ros acknowledge the research initiation grant received from the Universidad Politécnica de Cartagena (UPCT). Victor Blanco acknowledges the financial support received for postdoctoral training (Post-doctoral Fellowship 21261/PD/19) from the Fundación Séneca, Comunidad Autónoma de la Región de Murcia (Spain).

Acknowledgments: The authors are grateful to the staff of the “Tomás Ferro” Experimental Agro-food Station of the Universidad Politécnica de Cartagena for letting them use their facilities to carry out the study.

Conflicts of Interest: The authors declare no conflict of interest.

References

1. IPCC. IPCC Climate Change 2014: Synthesis Report. In *Contribution of Working Groups I, II and III to the Fifth Assessment Report of the Intergovernmental Panel on Climate Change*; Core Writing Team, Pachauri, R.K., Meyer, L.A., Eds.; IPCC: Geneva, Switzerland, 2014; p. 151.
2. Medrano, H.; Bota, J.; Abadía, A.; Sampol, B.; Escalona, J.M.; Flexas, J. Effects of drought on light-energy dissipation mechanisms in high-light-acclimated, field-grown grapevines. *Funct. Plant Biol.* **2002**, *29*, 1197–1207. [[CrossRef](#)] [[PubMed](#)]
3. Oraee, A.; Tehranifar, A. Evaluating the potential drought tolerance of pansy through its physiological and biochemical responses to drought and recovery periods. *Sci. Hortic.* **2020**, *265*, 109225. [[CrossRef](#)]

4. Chaves, M.M.; Miguel Costa, J.; Madeira Saibo, N.J. Recent advances in photosynthesis under drought and salinity. In *Plant Responses to Drought and Salinity Stress*, 1st ed.; Turkan, I., Ed.; Academic Press: Cambridge, MA, USA, 2011; Volume 57, pp. 49–104, ISBN 9780123876928.
5. Puértolas, J.; Pardos, M.; De Ollas, C.; Albacete, A.; Dodd, I.C. Soil moisture heterogeneity regulates water use in *Populus nigra* L. by altering root and xylem sap phytohormone concentrations. *Tree Physiol.* **2020**, *40*, 762–773. [[CrossRef](#)] [[PubMed](#)]
6. Chaves, M.M.; Maroco, J.P.; Pereira, J.S. Understanding plant responses to drought—From genes to the whole plant. *Funct. Plant Biol.* **2003**, *30*, 239–264. [[CrossRef](#)]
7. FAOSTAT FAO—Food and Agriculture Organization of the United Nations. Statistics Division. 2019. Available online: <http://www.fao.org/faostat/en/#data/QC/visualize> (accessed on 3 June 2021).
8. Marsal, J.; Lopez, G.; del Campo, J.; Mata, M.; Arbones, A.; Girona, J. Postharvest regulated deficit irrigation in ‘Summit’ sweet cherry: Fruit yield and quality in the following season. *Irrig. Sci.* **2010**, *28*, 181–189. [[CrossRef](#)]
9. Blaya-Ros, P.J.; Blanco, V.; Domingo, R.; Soto-Valles, F.; Torres-Sánchez, R. Feasibility of low-cost thermal imaging for monitoring water stress in young and mature sweet cherry trees. *Appl. Sci.* **2020**, *10*, 5461. [[CrossRef](#)]
10. Blanco, V.; Torres-Sánchez, R.; Blaya-Ros, P.J.; Pérez-Pastor, A.; Domingo, R. Vegetative and reproductive response of ‘Prime Giant’ sweet cherry trees to regulated deficit irrigation. *Sci. Hortic.* **2019**, *249*, 478–489. [[CrossRef](#)]
11. Blanco, V.; Blaya-Ros, P.J.; Torres-Sánchez, R.; Domingo, R. Influence of regulated deficit irrigation and environmental conditions on reproductive response of sweet cherry trees. *Plants* **2020**, *9*, 94. [[CrossRef](#)] [[PubMed](#)]
12. Blanco, V.; Martínez-Hernández, G.B.; Artés-Hernández, F.; Blaya-Ros, P.J.; Torres-Sánchez, R.; Domingo, R. Water relations and quality changes throughout fruit development and shelf life of sweet cherry grown under regulated deficit irrigation. *Agric. Water Manag.* **2019**, *217*, 243–254. [[CrossRef](#)]
13. Farooq, M.; Hussain, M.; Wahid, A.; Siddique, K.H.M. Drought stress in plants: An overview. In *Plant Responses to Drought Stress: From Morphological to Molecular Features*; Springer: Berlin/Heidelberg, Germany, 2012; Volume 9783642326, pp. 1–33, ISBN 9783642326530.
14. Castel, J.R.; Fereres, E. Responses of young almond trees to two drought periods in the field. *J. Hortic. Sci.* **1982**, *57*, 175–187. [[CrossRef](#)]
15. Torrecillas, A.; Galego, R.; Pérez-Pastor, A.; Ruiz-Sánchez, M.C. Gas exchange and water relations of young apricot plants under drought conditions. *J. Agric. Sci.* **1999**, *132*, 445–452. [[CrossRef](#)]
16. Ruiz-Sánchez, M.C.; Domingo, R.; Torrecillas, A.; Pérez-Pastor, A. Water stress preconditioning to improve drought resistance in young apricot plants. *Plant Sci.* **2000**, *156*, 245–251. [[CrossRef](#)]
17. Bhusal, N.; Lee, M.; Lee, H.; Adhikari, A.; Han, A.R.; Han, A.; Kim, H.S. Evaluation of morphological, physiological, and biochemical traits for assessing drought resistance in eleven tree species. *Sci. Total Environ.* **2021**, *779*, 146466. [[CrossRef](#)]
18. Abdelfatah, A.; Aranda, X.; Savé, R.; de Herralde, F.; Biel, C. Evaluation of the response of maximum daily shrinkage in young cherry trees submitted to water stress cycles in a greenhouse. *Agric. Water Manag.* **2013**, *118*, 150–158. [[CrossRef](#)]
19. Blanco, V.; Domingo, R.; Pérez-Pastor, A.; Blaya-Ros, P.J.; Torres-Sánchez, R. Soil and plant water indicators for deficit irrigation management of field-grown sweet cherry trees. *Agric. Water Manag.* **2018**, *208*, 83–94. [[CrossRef](#)]
20. Brito, C.; Dinis, L.; Moutinho-Pereira, J.; Correia, C.M. Drought stress effects and olive tree acclimation under a changing climate. *Plants* **2019**, *8*, 232. [[CrossRef](#)] [[PubMed](#)]
21. Livellara, N.; Saavedra, F.; Salgado, E. Plant based indicators for irrigation scheduling in young cherry trees. *Agric. Water Manag.* **2011**, *98*, 684–690. [[CrossRef](#)]
22. Turner, N.C. Turgor maintenance by osmotic adjustment: 40 years of progress. *J. Exp. Bot.* **2018**, *69*, 3223–3233. [[CrossRef](#)] [[PubMed](#)]
23. Ranney, T.G.; Bassuk, N.L.; Whitlow, T.H. Turgor maintenance in leaves and roots of ‘Colt’ cherry trees (*Prunus avium* x *pseudocerasus*) in response to water stress. *J. Hortic. Sci.* **1991**, *66*, 381–387. [[CrossRef](#)]
24. Allen, R.G.; Pereira, L.S.; Raes, D.; Smith, M. FAO Irrigation and drainage paper. In *Crop. Evapotranspiration-Guidelines for Computing Crop. Water Requirements*; Food and Agriculture Organization: Rome, Italy, 1998; ISBN 9253042192.
25. Marsal, J. FAO irrigation and drainage paper. In *Crop. Yield Response Water. Sweet Cherry*; Food and Agriculture Organization: Rome, Italy, 2012; pp. 449–457, ISBN 978-9251072745.
26. Fereres, E.; Pruitt, W.O.; Beutel, J.A.; Henderson, D.W.; Holzapfel, E.; Schulbach, H.; Uriu, K. Evapotranspiration and drip irrigation scheduling. In *Drip Irrigation Management*; Leaflet 21259; Division of Agricultural Sciences, University of California: Los Angeles, CA, USA, 1981; pp. 8–13.
27. Turner, N.C. Measurement of plant water status by the pressure chamber technique. *Irrig. Sci.* **1988**, *9*, 289–308. [[CrossRef](#)]
28. Hsiao, T.C. Measurements of plant water status. *Agronomy* **1990**, *30*, 243–279.
29. McCutchan, H.; Shackel, K.A. Stem-water potential as a sensitive indicator of water stress in prune trees (*Prunus domestica* L. cv. French). *J. Am. Soc. Hortic. Sci.* **1992**, *117*, 607–611. [[CrossRef](#)]
30. Gucci, R.; Xiloyannis, C.; Flore, J.A. Gas exchange parameters, water relations and carbohydrate partitioning in leaves of field-grown *Prunus domestica* following fruit removal. *Physiol. Plant.* **1991**, *83*, 497–505. [[CrossRef](#)]
31. Turner, N.C. Techniques and experimental approaches for the measurement of plant water status. *Plant Soil* **1981**, *58*, 339–366. [[CrossRef](#)]

32. Blanco, V.; Zoffoli, J.P.; Ayala, M. High tunnel cultivation of sweet cherry (*Prunus avium* L.): Physiological and production variables. *Sci. Hort.* **2019**, *251*, 108–117. [[CrossRef](#)]
33. Chaves, M.M.; Flexas, J.; Pinheiro, C. Photosynthesis under drought and salt stress: Regulation mechanisms from whole plant to cell. *Ann. Bot.* **2009**, *103*, 551–560. [[CrossRef](#)]
34. Marsal, J.; Lopez, G.; Arbones, A.; Mata, M.; Vallverdu, X.; Girona, J. Influence of post-harvest deficit irrigation and pre-harvest fruit thinning on sweet cherry (cv. New Star) fruit firmness and quality. *J. Hort. Sci. Biotechnol.* **2009**, *84*, 273–278. [[CrossRef](#)]
35. Intrigliolo, D.S.; Castel, J.R. Vine and soil-based measures of water status in a Tempranillo vineyard. *Vitis J. Grapevine Res.* **2006**, *45*, 157–163. [[CrossRef](#)]
36. Domingo, R.; Ruiz-Sanchez, M.C.; Sánchez-Blanco, M.J.; Torrecillas, A. Water relations, growth and yield of Fino lemon trees under regulated deficit irrigation. *Irrig. Sci.* **1996**, *16*, 115–123. [[CrossRef](#)]
37. Martínez-Vilalta, J.; Poyatos, R.; Aguadé, D.; Retana, J.; Mencuccini, M. A new look at water transport regulation in plants. *New Phytol.* **2014**, *204*, 105–115. [[CrossRef](#)] [[PubMed](#)]
38. Fereres, E.; Cruz-Romero, G.; Hoffman, G.J.; Rawlins, S.L. Recovery of orange trees following severe water stress. *J. Appl. Ecol.* **1979**, *16*, 833–842. [[CrossRef](#)]
39. Conesa, M.R.; de la Rosa, J.M.; Domingo, R.; Bañón, S.; Pérez-Pastor, A. Changes induced by water stress on water relations, stomatal behaviour and morphology of table grapes (cv. Crimson Seedless) grown in pots. *Sci. Hort.* **2016**, *202*, 9–16. [[CrossRef](#)]
40. Mellisho, C.D.; Cruz, Z.N.; Conejero, W.; Ortuño, M.F.; Rodríguez, P. Mechanisms for drought resistance in early maturing cvar Flordastar peach trees. *J. Agric. Sci.* **2011**, *149*, 609–616. [[CrossRef](#)]
41. Bhusal, N.; Lee, M.; Reum Han, A.; Han, A.; Kim, H.S. Responses to drought stress in *Prunus sargentii* and *Larix kaempferi* seedlings using morphological and physiological parameters. *For. Ecol. Manag.* **2020**, *465*, 118099. [[CrossRef](#)]
42. Farooq, M.; Wahid, A.; Kobayashi, N.; Fujita, D.; Basra, S.M.A. Plant drought stress: Effects, mechanisms and management. *Agron. Sustain. Dev.* **2009**, *29*, 185–212. [[CrossRef](#)]
43. Vile, D.; Garnier, É.; Shipley, B.; Laurent, G.; Navas, M.L.; Roumet, C.; Lavorel, S.; Díaz, S.; Hodgson, J.G.; Lloret, F.; et al. Specific leaf area and dry matter content estimate thickness in laminar leaves. *Ann. Bot.* **2005**, *96*, 1129–1136. [[CrossRef](#)]
44. Egea, G.; Nortes, P.A.; González-Real, M.M.; Baille, A.; Domingo, R. Agronomic response and water productivity of almond trees under contrasted deficit irrigation regimes. *Agric. Water Manag.* **2010**, *97*, 171–181. [[CrossRef](#)]
45. Sack, L.; John, G.P.; Buckley, T.N. ABA accumulation in dehydrating leaves is associated with decline in cell volume, not turgor pressure. *Plant Physiol.* **2018**, *176*, 489–493. [[CrossRef](#)]
46. Ivanov, A.A. Response of wheat seedlings to combined effect of drought and salinity. In *Stress Responses in Plants Mechanisms of Toxicity and Tolerance*; Springer International Publishing: Cham, Switzerland, 2015; pp. 159–198, ISBN 9783319133683.
47. Lawlor, D.W.; Cornic, G. Photosynthetic carbon assimilation and associated metabolism in relation to water deficits in higher plants. *Plant Cell Environ.* **2002**, *25*, 275–294. [[CrossRef](#)] [[PubMed](#)]
48. Ehleringer, J.; Forseth, I. Solar tracking by plants. *Science* **1980**, *210*, 1094–1098. [[CrossRef](#)] [[PubMed](#)]
49. Briglia, N.; Williams, K.; Wu, D.; Li, Y.; Tao, S.; Corke, F.; Montanaro, G.; Petrozza, A.; Amato, D.; Cellini, F.; et al. Image-based assessment of drought response in grapevines. *Front. Plant Sci.* **2020**, *11*, 1–12. [[CrossRef](#)] [[PubMed](#)]
50. Wu, N.; Zhang, Y.M.; Downing, A.; Aanderud, Z.T.; Tao, Y.; Williams, S. Rapid adjustment of leaf angle explains how the desert moss, *Syntrichia caninervis*, copes with multiple resource limitations during rehydration. *Funct. Plant Biol.* **2014**, *41*, 168–177. [[CrossRef](#)] [[PubMed](#)]
51. Hsiao, T.C. Plant responses to water stress. *Annu. Rev. Plant Physiol.* **1973**, *24*, 519–570. [[CrossRef](#)]
52. Puerto, P.; Domingo, R.; Torres, R.; Pérez-Pastor, A.; García-Riquelme, M. Remote management of deficit irrigation in almond trees based on maximum daily trunk shrinkage. Water relations and yield. *Agric. Water Manag.* **2013**, *126*, 33–45. [[CrossRef](#)]
53. Martínez-García, P.J.; Hartung, J.; de los Cobos, F.P.; Martínez-García, P.; Jalili, S.; Sánchez-Roldán, J.M.; Rubio, M.; Dicenta, F.; Martínez-Gómez, P. Temporal response to drought stress in several *Prunus* rootstocks and wild species. *Agronomy* **2020**, *10*, 1383. [[CrossRef](#)]